BIOCHEMISTRY
including biophysical chemistry & molecular biology

Article

pubs.acs.org/biochemistry

The Enzymatic Activity of Lipases Correlates with Polarity-Induced Conformational Changes: A Trp-Induced Quenching Fluorescence Study

Jakob Skjold-Jørgensen,[†,‡] Vikram K. Bhatia,[‡] Jesper Vind,[‡] Allan Svendsen,*[,‡] Morten J. Bjerrum,[†] and David Farrens[§]

[†]Department of Chemistry, University of Copenhagen, Universitetsparken 5, DK 2100 Copenhagen, Denmark

[‡]Novozymes A/S, Brudelysvej 35, DK 2880 Bagværd, Denmark

[§]Biochemistry & Molecular Biology, Oregon Health and Science University, 3181 Southwest Jackson Park Road, Portland, Oregon 97239, United States

Supporting Information

ABSTRACT: Triacylglycerol hydrolases (EC 3.1.1.3) are thought to become activated when they encounter the water−lipid interface causing a "lid" region to move and expose the catalytic site. Here, we tested this idea by looking for lid movements in *Thermomyces lanuginosus* lipase (TL lipase), and in variants with a mutated lid region of esterase (Esterase) and esterase/lipase (Hybrid) character. To measure lid movements, we employed the tryptophan-induced quenching (TrIQ) fluorescence method to measure how effectively a Trp residue on the lid of these mutants (at position 87 or 89) could quench a fluorescent probe (bimane) placed at nearby site 255 on the protein. To test if lid movement is induced when the enzyme detects a lower-polarity environment (such as at the water−lipid interface), we performed these studies in solvents with different dielectric constants (ε). The results show that lid movement is highly dependent on the particular lid residue composition and solvent polarity. The data suggest that in aqueous solution (ε = 80), the Esterase lid is in an "open" conformation, whereas for the TL lipase and Hybrid, the lid remains "closed". At lower solvent polarities (ε < 46), the lid region for all of the mutants is more "open". Interestingly, these behaviors mirror the structural changes thought to take place upon activation of the enzyme at the water−lipid interface. Together, these results support the idea that lipases are more active in low-polarity solvents because the lid adopts an "open" conformation and indicate that relatively small conformational changes in the lid region play a key role in the activation mechanism of these enzymes.

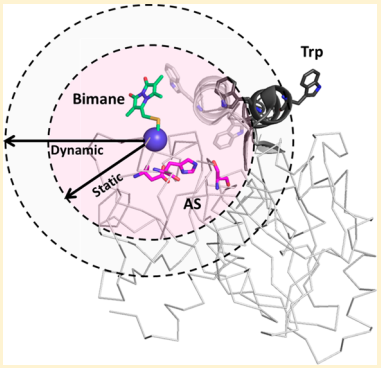

The nature of the activation mechanism in *Thermomyces lanuginosus* (TL lipase) lipases and related triacylglycerol hydrolases (EC 3.1.3) has been subject to comprehensive studies since the first crystal structures emerged in the early 1990s.[1−4] Like most lipases, TL lipase is dependent on a lipid interface to become activated and gain full catalytic function, a phenomenon termed interfacial activation.[5] Interfacial activation inherently represents one of the major issues for investigating the activation mechanism in triacyl-hydrolase lipases because catalysis takes place at the boundary between water and lipid. The general consensus from a number of studies (including *in vitro* experiments,[6] site-directed mutagenesis,[7−9] X-ray crystal structures,[3,10] MD simulations,[11−13] site-directed spin labeling,[14−16] and intrinsic tryptophan fluorescence studies[17−19]) is that a small, secondary structural motif forms a "lid" over the catalytic cleft, and this lid plays a key role in the activity, specificity, and activation mechanism of TL lipase and related lipases.[6,8,15,16,20−22] The lid region, an α-helical domain with two hinge domains posterior and anterior relative to the α-helix, covers the active site of TL lipase in a homogeneous aqueous solution, thus keeping the lipase catalytically inactive. As the lipase encounters an interface, the lid opens, exposing a large hydrophobic patch around the active site corresponding to ∼8% (800 Å^2) of the total protein surface area.[23]

Ferulic acid esterase from *Aspergillus niger* (FAEA) is structurally very similar to TL lipase.[24] However, FAEA is active on water-soluble substrates and does not display lipase activity.[25] Previous studies have shown that the activation mechanism in TL lipase can be altered by changing the lid residue composition based on the primary sequence of the lid in FAEA.[6] Variants with a FAEA-like lid region, spanning 17 residues, have been shown to be active on water-soluble substrates and display activation at the lipid interface faster than that of TL in both activity and fluorescence studies. Such findings suggest that changes in the lid residue composition allow the lipase to adopt an open lid conformation in a homogeneous aqueous solution, which is energetically feasible.

Received: March 27, 2015
Revised: June 18, 2015
Published: June 18, 2015

DOI: 10.1021/acs.biochem.5b00328
Biochemistry 2015, 54, 4186−4196

From structural studies of TL lipase with an inhibitor bound in the active site pocket, it is known that the lid displaces itself from the active site upon activation.[10] However, this conformational change represents a relatively small movement of ~10 Å between the closed and open state of the lid [measured from the center point of the α-helix in Protein Data Bank (PDB) entries 1DT3 and 1EIN,[10] respectively]. This delicate movement in TL lipase and related lipases is thus difficult to probe using fluorescence-based methods such as Förster resonance energy transfer (FRET), where energy transfer efficiency commonly reaches 100% at distances between the donor and acceptor of <20 Å.[26]

Recent developments in the field of site-directed fluorescence labeling (SDFL) have made it possible to overcome this problem and investigate the dynamics of proteins within the range of 7−15 Å. One such approach employs either tryptophan-induced quenching (TrIQ) or tyrosine-induced quenching (TyrIQ) to certain fluorescent probes,[27,28] processes that occur efficiently only in the distance range of 7−15 Å, presumably through a photoinduced electron transfer (PET) process.[29,30]

In this study, we used the TrIQ method[27] to investigate the activation mechanism of TL lipase and certain lid variants with FAEA character. Two hypotheses were tested: (1) Lipase activation (lid opening) is triggered when the dielectric constant of the solvent is lowered, and (2) differences exist in the open and closed states of the lid between TL lipase and FAEA-based lid variants. Below, we present and discuss our results of testing these hypotheses using the TrIQ method on lid variants of TL lipase labeled with the fluorescent probe monobromobimane (mBBr), studied with steady state and time-correlated single-photon counting (TCSPC) fluorescence spectroscopy.

MATERIALS AND METHODS

Materials. Unless designated, all reagents and biochemical supplies were purchased from Sigma-Aldrich and affiliates.

Engineering of Lid Variants. Lid variants were designed on the basis of the lid residue composition in *A. niger* ferulic acid esterase (FAEA), *T. lanuginosus* (TL) lipase, and related hydrolases as previously described, spanning 17 residues[6] (see the primary sequence alignment of lid residues in each variant in Figure S1 of the Supporting Information). For all variants, a cysteine residue was specifically introduced by mutation into the protein sequence at site I255 (in front of the lid), thus allowing specific site-directed fluorescence labeling with the cysteine reactive fluorophore mBBr.

Variant Construction, Transformation, and Screening. All variant genes were generated by spliced overlap extension (SOE) polymerase chain reaction[31] as previously described.[6] The lipase variant genes were inserted into a cloning plasmid, and purified DNA was sequenced across the whole gene, transformed into an *Aspergillus oryzae* strain, and fermented according to previous methods.[32] Protoplasts were stored at −80 °C and thawed when needed. Expression was verified by sodium dodecyl sulfate−polyacrylamide gel electrophoresis (SDS−PAGE) using SimplyBlue Safestain (Life Technologies, catalog no. LC6065). Variant screening was performed for successfully transformed *A. oryzae* strains using a standard pNP-valerate activity assay.[33]

Purification. Expression and purification of lipase variants were performed according to previous protocols[6,34] using hydrophobic interaction and anion-exchange chromatography methods. Variants were purified to a high degree with no observable contaminants verified by SDS−PAGE. All samples were buffer-exchanged and concentrated in 50 mM 3-propanesulfonic acid (MOPS) (pH 7.5) using centrifugal filter units (Ultracel-10K, Millipore).

Intact Molecular Weight Analysis. The intact molecular weight of each lipase mutant was determined by liquid chromatography−electrospray ionization mass spectrometry (LC−ESI-MS) analysis using a MAXIS II electrospray mass spectrometer (Bruker Daltonik GmbH, Bremen, Germany). All samples were diluted to ~0.5 mg/mL in Milli-Q water. For the MS analysis of all variants, the sulfhydryl group of the introduced cysteine residue was blocked by disulfide coupling to free cysteine (presumably during protein expression[34]). The intact molecular weights were determined for untreated samples, reduced samples, and bimane-labeled samples. Reduced samples were treated with 0.5 mM tris(2-carboxyethyl)phosphine (TCEP) to remove cysteine-reacted species. Samples were applied to an Aeris Widepore C4 column (Phenomenex), washed and eluted running an acetonitrile linear gradient, and introduced into the electrospray source with a flow of 300 mL/min by an Ultimate 3000 LC system (Dionex). Data analysis was performed with DataAnalysis version 4.2 (Bruker Daltonik GmbH). Intact molecular weights of the untreated, reduced, and labeled samples are shown in Table S1 and Figure S2 of the Supporting Information.

Solvent-Exposed Hydrophobic Surface Area (SEHSA) Assay. The solvent-exposed hydrophobic surface area for each variant (unlabeled) was investigated using 1-anilinonaphthalene-8-sulfonic acid (ANS) as an extrinsic fluorophore, as previously described.[6] In brief, a 0.2 mg/mL sample was mixed with 0.25 mM ANS in 25 mM MOPS (pH 7.5). The degree of ANS fluorescence was measured with excitation at 380 nm and emission collected from 400 to 650 nm. Excitation and emission slit widths were 10 nm. Measurements were recorded on a fluorescence spectrometer at room temperature (PerkinElmer, LS50B) in a quartz cuvette (Hellma QS 105.250). An average of three consecutive emission scans were taken for each measurement. All samples were reduced with ~0.5 mM TCEP prior to analysis to remove any cysteine-reacted species.

Labeling of Lipase Variants. Variants were labeled with monobromobimane (mBBR). All samples were diluted to 15 μM in 25 mM MOPS (pH 7.6) (buffer A); 250 μL of a protein sample was purged with argon to remove oxygen from the solution. A 10-fold molar excess of TCEP was added to each protein sample and gently mixed. The samples were incubated for 10−20 min at room temperature. mBBR was subsequently added in a 15-fold molar excess, and samples were incubated overnight at 4 °C or for 3−4 h at room temperature on a shaker bed in the dark. The reaction mix was subjected to gel filtration using NAP-5 (GE Healthcare) columns equilibrated with buffer A. Excess dye was removed by five repeated concentration and dilution steps in buffer A using Amicon Concentrators (10K molecular weight cutoff, AMICON ULTRA). The labeling efficiency was determined from measurements of the absorbance spectrum of each variant (Shimadzu UV 1601), and calculated assuming an extinction coefficient for bimane of 5000 M^{-1} cm^{-1}. The concentration of protein was calculated using extinction coefficients of 35560 M^{-1} cm^{-1} for TL lipase (Lipase)-based variants, 36840 M^{-1} cm^{-1} for Hybrid-based variants, and 31150 M^{-1} cm^{-1} for Esterase-based variants. For Trp mutants, the extinction coefficient at 280 nm was increased

DOI: 10.1021/acs.biochem.5b00328
Biochemistry 2015, 54, 4186−4196

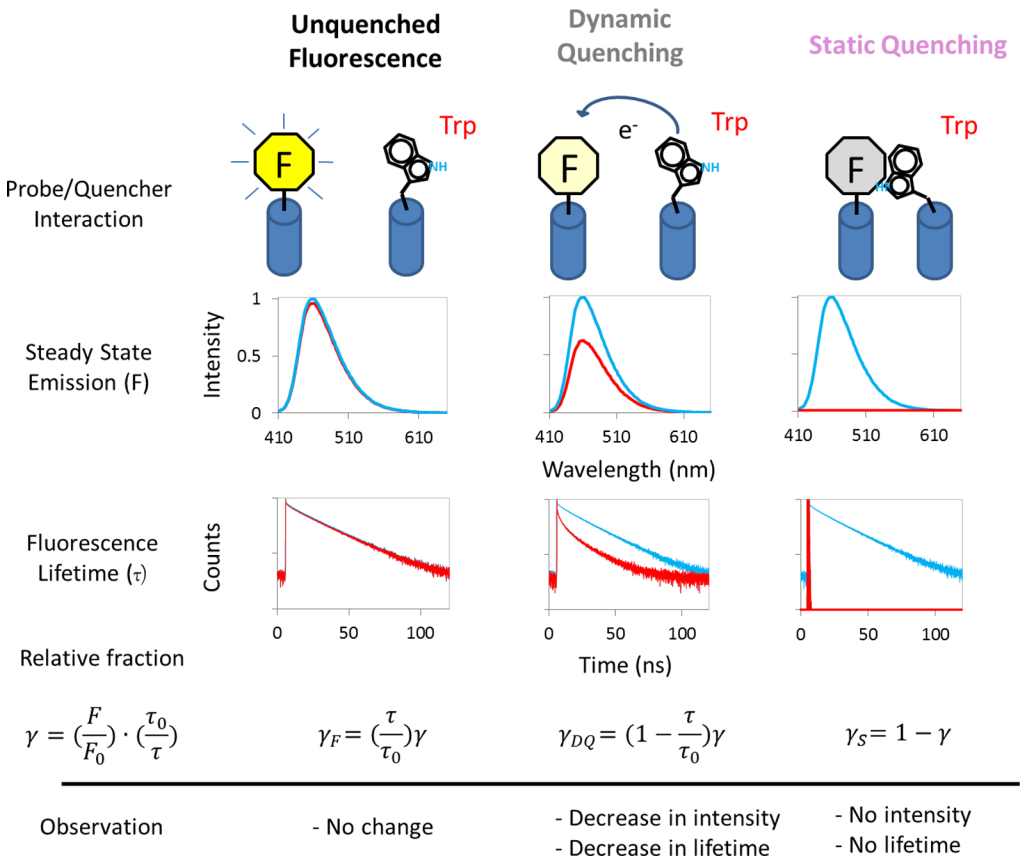

Figure 1. TrIQ analysis assumes that three possible fluorescent behaviors can be caused by different interactions between the quencher (Trp) and fluorophore (bimane). F, F_0, τ, and τ_0 represent the fluorescence intensities and lifetimes of the sample with (red line) and without a Trp (blue line) in the lid, respectively. The fraction of fluorescence originating from a noncomplexed conformation is determined from $\gamma = (F/F_0)(\tau_0/\tau)$. This fraction of fluorophores emits photons through either unquenched [$\gamma_F = (\tau/\tau_0)\gamma$, left] or dynamically quenched fluorescence [$\gamma_{DQ} = (1 - \tau/\tau_0)\gamma$, middle]. For unquenched fluorescence, the emission intensity and lifetime are unchanged. For dynamic quenching, both the intensity and the lifetime decrease. The nonfluorescent fraction of fluorophores that form a ground state complex with the quencher (Trp) results in "static quenching" ($1 - \gamma$, right). It is important to note that at any time, a snapshot of an ensemble of molecules may report a mixture of these possible states.

by 5690 M^{-1} cm^{-1}. The labeling efficiency was between 25 and 70%. Less than 5% unspecific labeling was observed using wild-type TL lipase (with no free, surface-exposed cysteine) as a negative control.

Variant Nomenclature and Structural Models. The variants were named according to their specific lid residue characteristics, e.g., Lipase, Esterase, or Hybrid. Unless specifically designated, all variants described are labeled with bimane at position C255. The location of the Trp residue in the lid region is explicitly stated in the name of each variant. For example, Esterase_W89 refers to a variant with an esterase lid labeled at site C255 and a Trp at position 89.

UV−Visible. An absorbance spectrum from 250 to 700 nm (Shimadzu UV 1601) was measured for each variant, and spectral shifts were investigated for signs of ground state complex formation (and thus static quenching) between the Trp (quencher) and bimane fluorophore[35] (Figure S2 of the Supporting Information).

Determining the Amount of Free Label. The amount of free, nonreacted label in each sample was assessed using a trichloroacetic acid (TCA) precipitation protocol, as previously described,[36] which measures the amount of nonattached, "free" fluorescent label remaining in a sample after precipitating the protein with TCA. In brief, 100 μL of a 10% TCA solution was added to a 100 μL protein sample. The sample was then incubated on ice for 30 min and subsequently centrifuged at 13000 rpm and 4 °C for 20 min. The integrated fluorescence emission spectrum was measured before and after centrifugation after buffer subtraction (Figure S4 of the Supporting Information). Use of this assay indicated that, in all cases, the amount of free label in our samples was <5%.

Thermal Stability. The thermal stability assay was performed as previously described.[6,37] In brief, SYPRO Orange (SO) (catalog no. S5692, 5000× stock concentrate) was diluted 250 times in a buffer comprising 50 mM MOPS (pH 7.5). Subsequently, 15 μL of dye solution was added to 15 μL of the 0.30 mg/mL protein sample. Melting curves for each variant before and after labeling were determined (using a StepOnePlus Real Time PCR System (Applied Biosystems)) running a temperature gradient from 25 to 96 °C at a scan rate of 76 °C/h with an initial 15 min reaction time at 25 °C.

Lipase Activity. To assess how the bimane label might impact the functional ability of the proteins, the hydrolytic activity toward pNP-palmitate embedded in a lipid layer of rendered, commercial pork fat (lard) (Dragsbæk A/S) at a 1:1 molar ratio was determined as previously described[6] for both the labeled and unlabeled mutants. The assay was conducted at 22 °C in 100 mM Tris and 2 mM $CaCl_2$ (pH 8) and the activity calculated from the steepest slope of the absorbance increase (at 405 nm) as a function of time.

DOI: 10.1021/acs.biochem.5b00328
Biochemistry 2015, 54, 4186−4196

Calculation of the Dielectric Constant in Solvent Mixtures. To estimate the dielectric constant of the solvent mixtures, Oster's rule[38] was applied to determine the polarization of a mixture of n components:

$$p_m = \frac{\sum_{i=1}^{n} x_i v_i p_i}{\sum_{i=1}^{n} x_i v_i} \quad (1)$$

where p_m is the polarization per unit volume and x, v, and p represent the mole fraction, the molar volume, and the polarization of pure component i, respectively. The polarization per unit volume is related to the dielectric constant by[39]

$$p = \frac{(\varepsilon - 1)(2\varepsilon + 1)}{9\varepsilon} \quad (2)$$

where p is the polarization per unit volume and ε is the dielectric constant of the fluid. From eqs 1 and 2, assuming that p equals p_m, the dielectric constant for each solvent was determined. Note that these calculations are only approximations and assume no volume change upon mixing. The calculated dielectric constants for the different solvent mixtures are listed in Table S2 of the Supporting Information.

Steady State Fluorescence Measurements. The fluorescence emission and excitation measurements were taken on a PTI fluorescence spectrometer in a T-format at 22 °C.

Excitation and emission slit widths were set to 4 and 12 nm, respectively. Experiments were conducted at 22 °C. Emission spectra were measured from 400 to 700 nm with excitation at 390 nm. Excitation spectra were taken from 250 to 410 nm while monitoring at the emission wavelength of 481 nm. Integrated steady state fluorescence emission intensities were calculated by integrating the fluorescence spectra from 410 to 700 nm. For measurements in ethanol/water mixtures, the integration range of 420−700 nm was used instead, because of increased scattering of the exciting light.

Fluorescence Lifetime Measurements. Fluorescence lifetime measurements were taken on a PicoQuant Fluo Time 200 time-correlated single-photon counting (TCSPC) instrument (PicoQuant, Berlin, Germany). A 405 nm pulsed diode laser was used as an excitation source, and the instrument response function (IRF) was 64 ps at full width at half-maximum (fwhm) for all measurements using a Ludox scattering solution. A minimum of 10000 photon counts were collected for every measurement. Emission was measured using a stacked long-pass filter of 470 nm. The fluorescence decay curves were fit using the FluoFit software (PicoQuant) and an exponential model to analyze the decay data:

$$I(t) = \sum_{i-1}^{n} A_i e^{-t/\tau_i}$$

where $I(t)$ is the fluorescence intensity, A_i is the amplitude of the ith component in counts, and τ_i is the lifetime of the ith component. The quality of the fits was evaluated using the value of χ^2, the residuals, and the autocorrelation function for each measurement. All measured bimane fluorescence lifetimes are listed in Table S3 of the Supporting Information for each variant.

Fluorescence Component Analysis. From the steady state and lifetime fluorescence measurements, the fluorescence components were calculated for each variant. The method for determining the different fluorescence contributions of each fluorophore−quencher pair has been previously described.[27,36,40] In short, the fraction (γ) of fluorophore and quencher in a nonstatic conformation is calculated by $\gamma = (F/F_0)(\tau_0/\tau)$. The contribution from these fluorescing species can be further separated as $\gamma = \gamma_F + \gamma_{DQ}$, where the contribution of fluorescence originating from unquenched fluorescence is defined as $\gamma_F = (\tau_0/\tau)\gamma$ and fluorescence from species undergoing dynamic quenching as $\gamma_{DQ} = (1 - \tau/\tau_0)\gamma$. The fraction of static quencher−fluorophore pairs (γs) is simply determined from $1 - \gamma$.

As shown in Figure 1, these calculations are used to quantify the relative fluorescence contributions corresponding to the three different possible fates of the Trp−fluorophore interaction. In the first scenario, unquenched fluorescence (γ_F), the fluorophore does not interact with the Trp quencher and thus there is no impact on the fluorescence signal. In the second scenario, dynamic quenching (γ_{DQ}), the Trp residue interacts with and quenches the fluorescence of the fluorophore during its excited state lifetime. This interaction causes both the fluorescence intensity and lifetime to decrease. The third scenario, static quenching (γs), occurs when the Trp and the fluorophore have formed a nonfluorescent ground state complex, even before the absorption of light by the fluorophore.

Circular Dichroism Spectroscopy. Circular dichroism (CD) spectroscopy was applied to investigate the structural stability of TL lipase, Lipase_W87, and Esterase_W89 in water/ethanol solvent mixtures of 0−90% (v/v) ethanol. A J-815 CD spectrometer (Jasco) was used to record CD spectra. Spectra were recorded in 10 mM Tris buffer (pH 7.5) with a protein concentration of 1 mg/mL. A quartz round cell for far-UV CD with a light path of 0.05 mm was used. CD spectra were collected from 260 to 180 nm with 1 nm intervals. A minimum of 10 scans were taken for each sample with a scan speed of 100 nm/min. Within a given experiment with varying ethanol concentrations, all samples had identical protein concentrations. The relative CD intensity as a measure of the secondary structure was calculated at each ethanol concentration for each variant by

$$\mathrm{RI}(\theta) = \frac{\theta_{192nm}(\text{mixture}) - \theta_{209nm}(\text{mixture})}{\theta_{192nm}(\text{water}) - \theta_{209nm}(\text{water})} \quad (3)$$

where θ(mixture) refers to the absorbance intensity at a given ethanol/water mixture at 192 and 209 nm and θ(water) is the absorbance intensity for the measured sample in water alone at these wavelengths. The spectra were averaged, and blanks were subtracted. Full CD spectra are shown in Figure S5 of the Supporting Information.

RESULTS

The Solvent-Exposed Hydrophobic Surface Area (SEHSA) Is Different between Lid Variants. To investigate the open versus closed state of the lid in each variant in aqueous solution, the solvent-exposed hydrophobic surface area was determined using ANS as an extrinsic fluorophore (Figure 2). When ANS binds to a hydrophobic, nonpolar surface area on a protein, its fluorescence quantum yield increases with a pronounced blue shift in fluorescence maximum.[41] As seen from the crystal structures of TL lipase with the lid in its closed and open conformation, lid opening reveals a large hydrophobic patch around the active site to the solvent (Figure 2A). From the fluorescence emission spectra (Figure 2B), it was evident that Lipase_W89 and Hybrid_W89 showed a very low

DOI: 10.1021/acs.biochem.5b00328
Biochemistry 2015, 54, 4186−4196

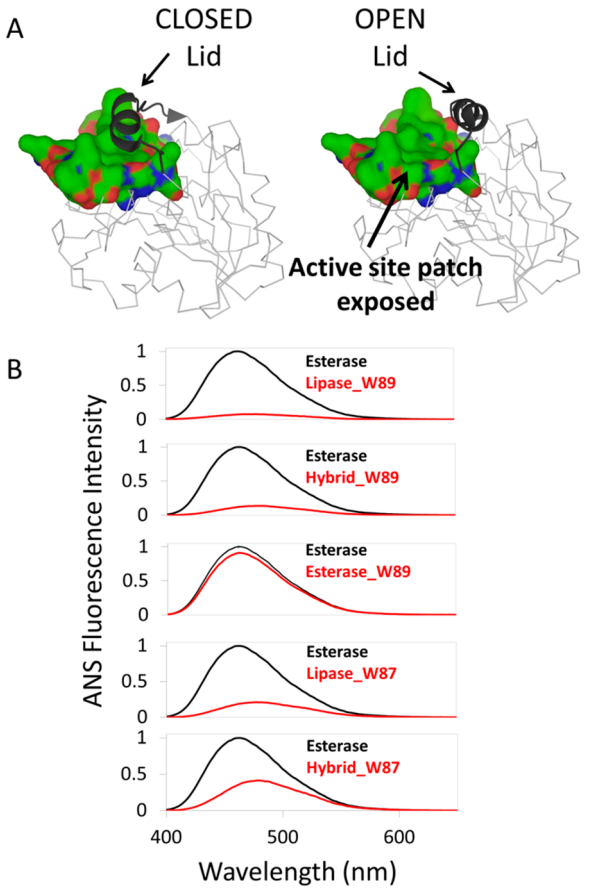

Figure 2. Lipase variants show different amounts of solvent-exposed hydrophobic surface area (SEHSA), as indicated by differential binding of the fluorophore ANS. (A) Models of TL lipase showing the hydrophobic patch around the active site that becomes exposed upon movement of the lid region (residues 82−98) from its closed to its open conformation (PDB entries 1DT3 and 1EIN, respectively,[10] black α-helices, surface representation; oxygen, red; nitrogen, blue; carbon, green, residues 146−152, 172−179, 201−217, and 251−258). (B) Fluorescence emission spectra of ANS when added to a solution of a 0.2 mg/mL protein sample. The spectra for each variant (red line) were normalized to the fluorescence intensity from ANS binding to Esterase (black line). Fluorescence measurements were conducted in 25 mM MOPS (pH 7.5).

degree of ANS fluorescence, indicative of a low degree of ANS binding. In contrast, Esterase and Esterase_W89 showed a marked increase in ANS fluorescence and a fluorescence maximum at 463 and 462 nm, respectively, which was substantially blue-shifted compared to the value of 478 nm detected for the other variants (Table S4 of the Supporting Information). Together, these results suggest that the ANS probe is strongly bound to a nonpolar site in Esterase and Esterase_W89 indicative of an open lid conformation, exposing the active site. Conversely, Lipase_W89, Lipase_W87, Hybrid_W89, and Hybrid_W87 supposedly have a closed lid conformation, shielding the active site from ANS binding. These results are in accordance with previous studies showing that TL lipase mutants containing a lid region from FAEA are active on water-soluble substrates ascribed to an open lid conformation.[6]

Structural Models Predict That the Open/Closed State of the Lid Will Produce Different Amounts of TrIQ for a Bimane Label on C255 and Trp at Site 87 or 89. To further investigate the open/closed state of the lid in each lipase mutant, two structural models were investigated using the TrIQ method (Figure 3). The first model involves variants with a Trp

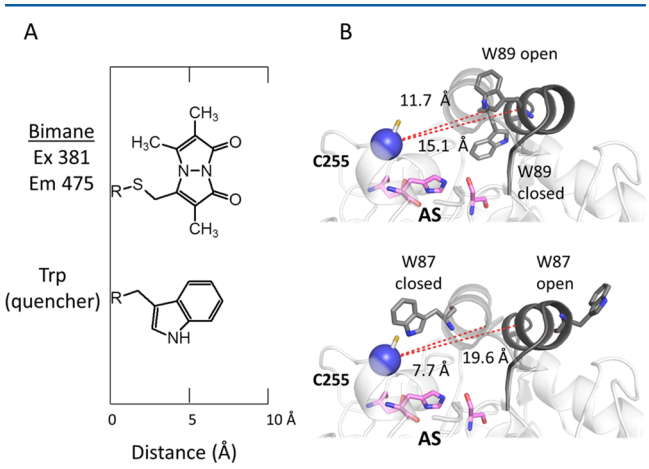

Figure 3. Model for investigating the activation (lid opening) in TL lipase using TrIQ. (A) Structural characteristics of bimane and Trp (quencher) showing the excitation and emission maxima for bimane. (B) Theoretical models of the open/closed states of the lid (gray and black cartoon, PDB entries 1EIN and 1DT3, respectively[10]), showing how a Trp located at position 89 (B, top) or 87 (B, bottom) reorients. The respective C_α−C_α distances between the C255 labeling site (blue sphere, sulfhydryl group in white sticks) and Trp (gray sticks) are also shown. The lid covers the active site in the closed state and upon activation moves to expose the active site (AS) triad (magenta lines, His258, Ser146, and Asp201).[53]

residue at position 89 (the native location of the Trp residue in TL lipase) in the α-helical domain of the lid region (Figure 3B, top). This site was chosen because the lid, in its closed state, covers the active site with Trp89 buried in the hydrophobic, active site pocket. Upon activation and lid opening, the Trp89 reorients and becomes exposed to the solvent.[17,42] During this rearrangement, the C_α−C_α distance between labeling site C255 and Trp89 changes by only ∼11.7 Å, to 15.1 Å.

The second model involves variants in which a Trp was introduced into the backbone at position 87 (Figure 2B, bottom). The site was chosen on the basis of earlier computational studies of the activation of TL lipase, showing that Glu87, the native residue at that site, undergoes a large displacement between the closed and open state of the lid.[12] Hence, these variants should allow better resolution of the open/closed states of the lid upon activation. In a closed conformation, the C_α−C_α distance between Trp and bimane is <8 Å, and in the fully open conformation, the C_α−C_α distance increases to ∼20 Å, outside Trp's empirically determined "sphere of quenching".[27]

Labeling with Bimane Does Not Perturb the Thermal Stability or Hydrolytic Activity between Labeled and Unlabeled Samples. We assessed the impact of bimane labeling on the thermal stability and enzymatic activity for all variants. Thermal scans and enzymatic activity assays did not indicate any severe perturbations caused by the labeling of the samples with bimane. It should be noted that the engineered variants showed a thermal stability decrease of up to 17 °C compared to that of wild-type TL lipase (Figure S6 of the Supporting Information). These results were expected, because previous studies have found that multiple mutations in the lid region significantly lower the thermal stability. However,

DOI: 10.1021/acs.biochem.5b00328
Biochemistry 2015, 54, 4186−4196

despite this decrease in stability, the lid variants remain structurally intact, as determined by far-UV circular dichroism,[6] and the spectra in Figure S5 of the Supporting Information.

Differences in the Open/Closed Conformation of the Lid among Lipase, Hybrid, and Esterase Are Detected by TrIQ. Steady state fluorescence emission spectra for each bimane-labeled mutant were determined in a homogeneous aqueous solution (Figure 4A). Interestingly, as shown below, it

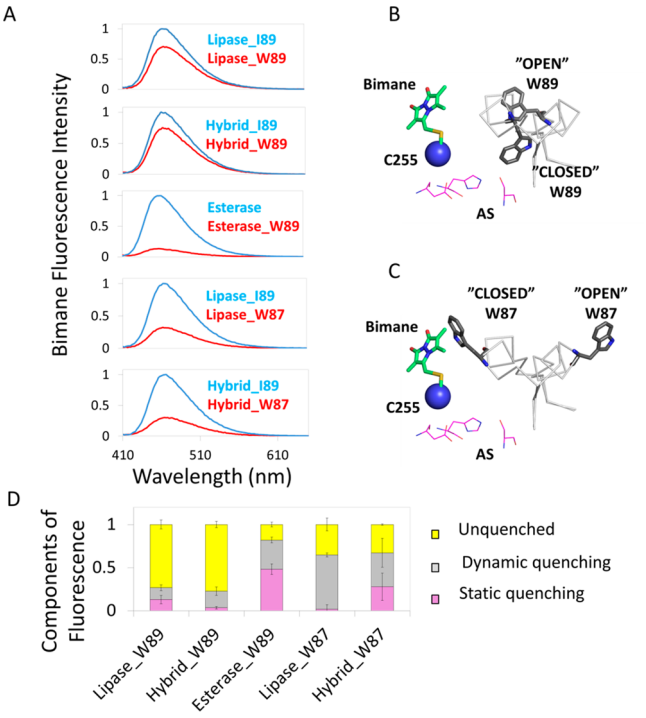

Figure 4. TL lipase lid variants show different amounts of lid opening in aqueous buffer as indicated by comparison of TrIQ data. (A) Fluorescence emission spectra of bimane labeled at position C255 in TL lipase lid variants of Lipase, Hybrid, or Esterase lid character (red line) with Trp (W) at position 89 or 87. The spectra from matched samples were normalized to their Trp-less controls (blue line). Spectra represent an average of three consecutive measurements. (B) Structural model of TL lipase labeled with bimane (green sticks) at C255 (blue sphere) showing the lid in its closed and open conformations (gray ribbon, PDB entries 1DT3 and 1EIN, respectively) with the predicted location of Trp at position 89 or (C) 87 (black sticks). The active site (AS) residues are shown as pink lines.[53] (D) The components of fluorescence for the different lid variants labeled at site C255 with bimane showing the contribution from unquenched (yellow), dynamic (gray), and static (purple) quenching in each sample. Error bars denote the standard deviation from two separate experiments. Fluorescence measurements were conducted in 25 mM MOPS (pH 7.5) at 22 °C.

is the ability of the exposed Trp89 to make direct contact with bimane that dominates how much quenching is observed, more so than simply the change in the Trp−bimane C_α−C_α distance. Lipase_W89 and Hybrid_W89 showed 70−80% relative bimane fluorescence intensity compared to those of their Trp-less controls, suggesting only a weak interaction between Trp89 and the bimane probe. On the other hand, Esterase_W89 (containing a lid region similar to that of FAEA, but with a Trp at position 89) showed a high degree of quenching with the fluorescence intensity reduced to ∼20% indicating a very intimate interaction between Trp and bimane (Figure 4B). For Lipase_W87 and Hybrid_W87, the relative fluorescence intensities were ∼35%, suggesting a close interaction with bimane (Figure 4C).

To resolve the different quenching components in each sample (e.g., unquenched, dynamic, and static quenching), we next measured fluorescence lifetimes for the samples and analyzed these along with the fluorescence emission intensity data (Figure 4D) to determine the fraction of dynamically and statically quenched fluorophores, as described in the legend of Figure 1. These analyses showed that Lipase_W89 and Hybrid_W89 exhibited around 20−30% quenching with dynamic quenching (15−30%) as the main component. For Esterase_W89, the quenching was mainly static in nature (∼50%), supporting the notion that bimane and Trp interact intimately. In Lipase_W87 and Hybrid_W87, the quenching component was chiefly represented by dynamic quenching (∼70%)

Conformational Changes in the Lid Region Occur in TL Lipase and Lid Variants When the Solvent Polarity Is Lowered. Lipases have long been known to function as catalysts in anhydrous environments,[43] and they are widely used in alcoholysis reactions to render alkyl esters for biodiesel production in the presence of triglycerides dissolved in methanol and ethanol.[44] This ability to function in different nonaqueous solvents has been investigated in several *in silico* and *in vitro* studies, showing that for TL lipase and related lipases[12,18,20,45,46] lid opening (activation) occurs, upon a lowering of the dielectric constant of the environment.

Here, we chose to investigate this phenomenon by measuring how the activation of the lipase variants depended on the polarity of the solvent in water/ethanol mixtures. The results show that, for Hybrid_W89 and Lipase_W89 (mutants with a Trp at position 89), the fluorescence decreased as the dielectric constant was lowered, indicative of increased TrIQ (Figure 5). Interestingly, the amount of fluorescence quenching increased substantially at ε = 46 and exhibited a high degree of static quenching for both variants. These results suggest that under these conditions, the Trp in Hybrid_W89 and Lipase_W89 comes into the proximity (and sometimes contact) of the bimane fluorophore attached to position C255 on the protein backbone during movement of the lid and exposure of the active site triad (Figure 5B).

Importantly, the high degree of fluorescence quenching seen for Esterase_W89 was sustained in all solvent mixtures, supporting the notion that the lid has an open conformation in aqueous buffer (ε ∼ 80) and remains open upon addition of ethanol. However, the unquenched component increased from ∼20 to ∼25% going from ε = 80 to ε = 46−30, indicating some perturbation of the bimane−Trp interaction. Interestingly, a significantly higher degree of quenching was observed for Hybrid_W89 than for Lipase_W89 at ε = 46−30, with 25 and 35% unquenched fluorescence remaining, respectively.

Fluorescence quenching was also investigated for Lipase_W87 and Hybrid_W87 with Trp at position 87, as a function of the dielectric constant (Figure 6). For these variants, the addition of ethanol resulted in large increases in fluorescence as the dielectric constant was lowered, an opposite trend in quenching compared to Lipase_W89 and Hybrid_W89. These results are consistent with Trp87 moving away from bimane at C255 during exposure of the active site triad (Figure 6B).

Lipase_W87 and Hybrid_W87 showed a very similar decrease in the extent of the Trp−bimane interaction as the

DOI: 10.1021/acs.biochem.5b00328
Biochemistry 2015, 54, 4186−4196

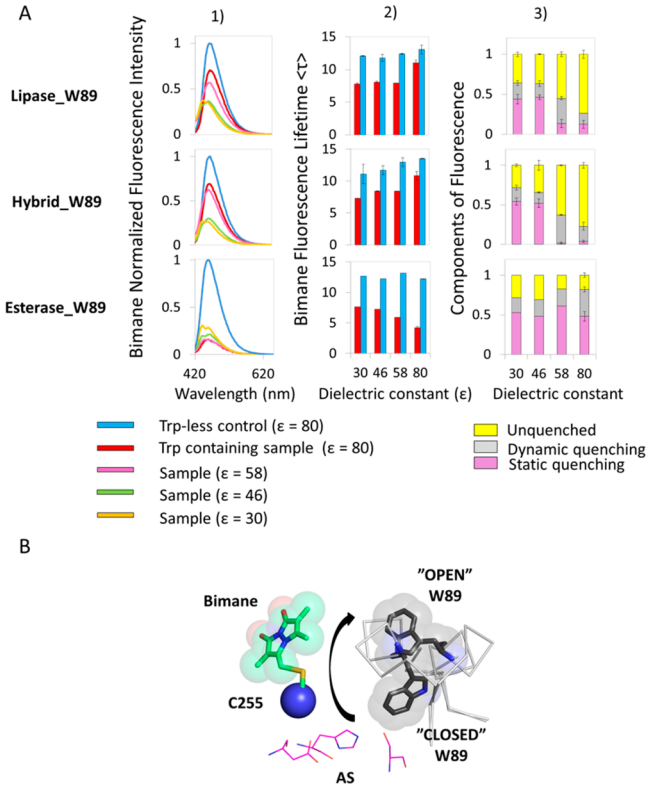

Figure 5. TrIQ data indicate lid opening correlates with the decreased dielectric constant of the solvent. (A) Bimane fluorescence emission spectra (1), average $\langle\tau\rangle$ fluorescence lifetimes (2), and fluorescence components (3) of Lipase_W89, Hybrid_W89, and Esterase_W89 determined in ethanol/water mixtures with the specified dielectric constants. The emission spectra of all variants showed a blue shift as solvent polarity decreased. For Lipase_W89 and Hybrid_W89, the fluorescence intensity decreased with a decrease in dielectric constant. For Esterase_W89, the intensity and lifetimes increased slightly as the dielectric constant was lowered. The average fluorescence lifetimes, $\langle\tau\rangle$, for each sample (red columns) and their Trp-less control (blue columns) were measured and used together with the emission intensity data to calculate the amount of static (purple), dynamic (gray), and unquenched fluorescence (yellow) for each sample, as described in the legend of Figure 1. Error bars denote the standard deviation from two independent measurements. Measurements were conducted at 22 °C. (B) Structural alignment of the open and closed conformations of the lid (residues 82−95; gray ribbon, PDB entries 1EIN and 1DT3, respectively) showing the expected location of the Trp89 residue (black sticks and translucent van der Waals radii) relative to the bimane fluorophore (green sticks and translucent van der Waals radii) attached at C255 (blue sphere). The active site triad (AS, Ser146, Asp201, and His258) is shown as pink sticks.

dielectric constant was lowered, with both nearly reaching the same fluorescence emission intensity and lifetime as their Trp-less controls at low solvent polarities, consistent with Trp's dwindling ability to quench as it moves away from the bimane probe at C255.

TL Lipase and Lid Variants Are Structurally Stable at High Ethanol Concentrations. We next assessed how the different ethanol/water solvent mixtures effected the structure of the lipase variants by measuring their CD spectra in solutions of 0−90% (v/v) ethanol (Figure S5 of the Supporting Information) and then comparing their calculated relative ellipticity to assess the effect on protein secondary structure (Figure 7).

Generally, the variants remained structurally intact up to a dielectric constant of $\varepsilon \sim 40$. Below this value, the CD signal intensities started to decrease and secondary structure signatures began to disappear. These stability measurements clearly show the lipase variants remain stable in relatively high concentrations of ethanol, and thus, the fluorescence quenching components determined above a dielectric constant of $\varepsilon = 40$ (e.g., dynamic, static, and unquenched fluorescence components) can reliably be used to interpret local conformational changes taking place in the vicinity of the bimane probe. Thus, our operational assumption is that the changes observed in the TrIQ are due to the dynamics of lid movements, and not to a globular protein unfolding event. However, this analysis also indicates the quenching measurements conducted at $\varepsilon = 30$ likely contain some fraction of unfolded or partially unfolded protein, and this caveat must be taken into account when interpreting the data.

An Activation Plot Shows the Amount of Open versus Closed Conformer in Each TL Lipase Mutant Varies with Solvent Polarity. To visualize and quantify differences in the amount of open versus closed conformers in each sample as a function of dielectric constant, we next used these data to construct an "activation plot" from the measured relative fluorescence emission intensities in the different water/ethanol mixtures (eqs 3 and 4 and Tables S5 and S6 of the Supporting Information). As seen from panels A and B of Figure 8, these plots show the lid movement associated with lipase activation began to occur at $\varepsilon \sim 50$ for all variants. Interestingly, at polarities below $\varepsilon = 46$, Hybrid_W89 nearly reached the same degree of quenching as seen for Esterase_W89, indicative of ~100% open conformers.

In contrast, although it shows a similar activation profile, Lipase_W89 did not activate to the same extent, with ~75% open conformers below $\varepsilon = 46$. These results indicate that Hybrid_W89 activates more favorably than Lipase_W89 at higher solvent polarities. These observations are consistent with previous studies showing that mutations in the lid region of TL lipase enhance activation and change the energy landscape of lid opening as a function of the dielectric constant.[6,12] As for Lipase_W87 and Hybrid_W87, the fluorescence emission intensity increased to a similar extent for both variants as the solvent polarity decreased. Although the lid residue compositions between Lipase_87 and Hybrid_W87 are distinctly different, with the latter containing partly FAEA character, the results suggest that they do not activate in a significantly different manner. Taken together, these results highlight the key role that the lid residue composition plays in the activation mechanism in TL lipase and related lipases.[20]

DISCUSSION

The TrIQ Data Suggest Two Modes in Which Lipase Activation Can Be Detected. Previous studies have empirically determined the nature of a "sphere of quenching" for certain probes that are sensitive to Trp- or Tyr-induced quenching (TrIQ or TyrIQ, respectively), that is, the sphere within which some fluorescent probes are sensitive to quenching by either of these residues.[27,28] In the specific case of Trp quenching bimane, the "sphere of quenching" has been empirically determined to be around 10−15 Å[27] for C_α−C_α distances between probe−quencher pairs situated on the same protein. Analysis of a model based on the TL lipase crystal structure clearly shows that the C_α−C_α distances between the bimane at position 255 and the Trp at position 89 are within

DOI: 10.1021/acs.biochem.5b00328
Biochemistry 2015, 54, 4186−4196

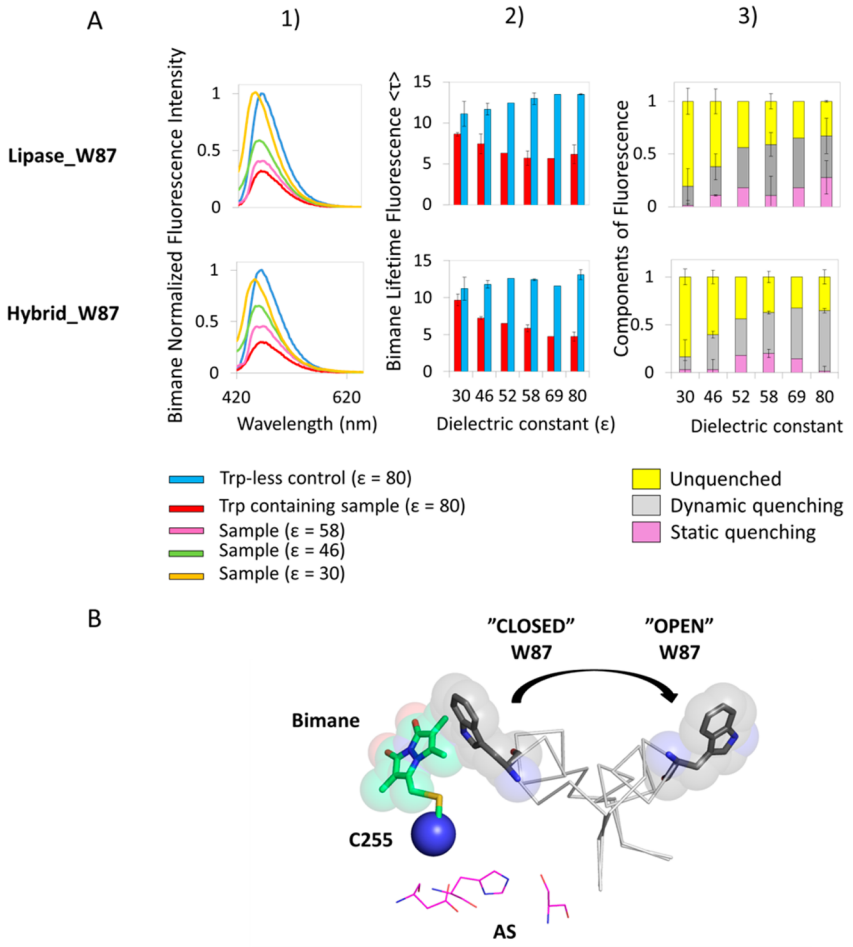

Figure 6. TrIQ data indicate TL lipase lid opening correlates with a decreased dielectric constant of the solvent. (A) Bimane fluorescence emission spectra (1), average ⟨τ⟩ lifetimes (2), and fluorescence components (3) of Lipase_W87 and Hybrid_W87 determined in ethanol/water mixtures with a specified dielectric constant. The λ_{max} of the emission spectra shows a blue shift with a decreasing solvent polarity. For Lipase_W87 and Hybrid_W87, the fluorescence intensity increased with a decrease in the dielectric constant. The fluorescence lifetimes, ⟨τ⟩, of each Trp mutant sample (red columns) and Trp-less control (blue columns) were also measured and used together with the emission intensity data to calculate the amount of static (purple), dynamic (gray), and unquenched fluorescence (yellow) for each sample. Error bars denote the standard deviation from two independent measurements. Measurements were conducted at 22 °C. (B) Structural alignment of the open and closed conformations of the lid (residues 82−95; gray ribbon, PDB entries 1EIN and 1DT3, respectively) showing the expected location of the Trp87 residue (black sticks and translucent van der Waals radii) relative to the bimane fluorophore (green sticks and translucent van der Waals radii) labeled at C255 (blue sphere). Residues in the active site triad (AS, Ser146, Asp201, and His258) are shown as pink sticks.

the sphere of quenching in the open and closed states of the lid (Figure 8B).

What then accounts for the large differences in quenching among Esterase_W89, Lipase_W89, and Hybrid_W89 we observe in a homogeneous aqueous solution? As indicated by the ANS assay, the lid in Esterase_W89 is likely in the open conformation, thus exposing Trp89 to the solvent, allowing it to make an intimate interaction with the bimane probe at position C255.

We describe this bimane−Trp interaction as an "I see you, I see you not" phenomenon. In the closed position, the Trp89 is largely out of sight of the bimane probe, because of it pointing inward, toward the active site pocket. However, when the lid opens, Trp89 becomes able to confront the bimane probe at C255, resulting in a high degree of bimane quenching (Figure 5B). This idea is supported by previous studies of the effect of stereochemistry on electron transfer rates between donor and acceptor molecules in organic model compounds (with the distance between the attachment sites of the donor and acceptor kept constant) showing that electron transfer rates can differ by orders of magnitude, depending on their respective geometric orientations.[47] In the case of Lipase_W87 and Hybrid_W87, the Trp is within the sphere of quenching in the closed state and moves outside the sphere upon opening (Figure 8C) in an "inside, outside" mode of action.

Impact of the Use of Ethanol in Studying Lipase Activation. In this study, we used ethanol to change the dielectric properties of the solvent mixtures in the TrIQ experiments. Because ethanol is known to impact the structure of water,[48] the properties of water/ethanol mixtures must be considered when assessing the fluorescence changes observed in the TrIQ experiments. Recall that our TrIQ data suggest activation of the lipase variants occurs at a dielectric constant of around ε = 50, corresponding to a mole fraction of 0.25 ethanol. Interestingly, Santucci and Onori found that ethanol forms microaggregates at a mole fraction of ethanol in water of 0.2.[48] Thus, it is tempting to speculate that microaggregates of ethanol play a role in the lipase activation we observe here. This interpretation would also explain the very small activation discrepancies observed between each variant investigated.

DOI: 10.1021/acs.biochem.5b00328
Biochemistry 2015, 54, 4186−4196

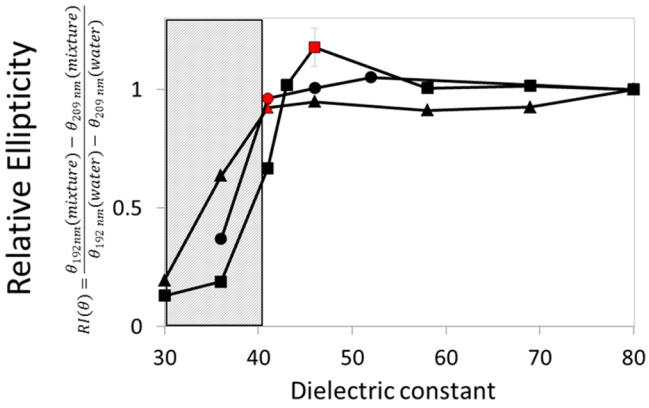

Figure 7. Relative ellipticity of TL lipase (wild type, triangles), Lipase_W87 (squares), and Esterase_W89 (circles) in water/ethanol mixtures as a function of the dielectric constant of the solvent. The buffer was 10 mM Tris (pH 7.5). Relative ellipticity was used as a measure of secondary structural stability using absorbance intensities at 192 and 209 nm. The measurements were conducted at room temperature. Ten scans were taken for each water/ethanol mixture with a scan speed of 100 nm/min for all samples. The concentration of protein within a given experiment was the same. Error bars denote the standard deviation of two measurements conducted with incubation for 3 h apart at the designated ethanol/water mixture. The raw data are reported in Figure S5 of the Supporting Information. The variants start to lose structural integrity below $\varepsilon \sim 40$ (gray box).

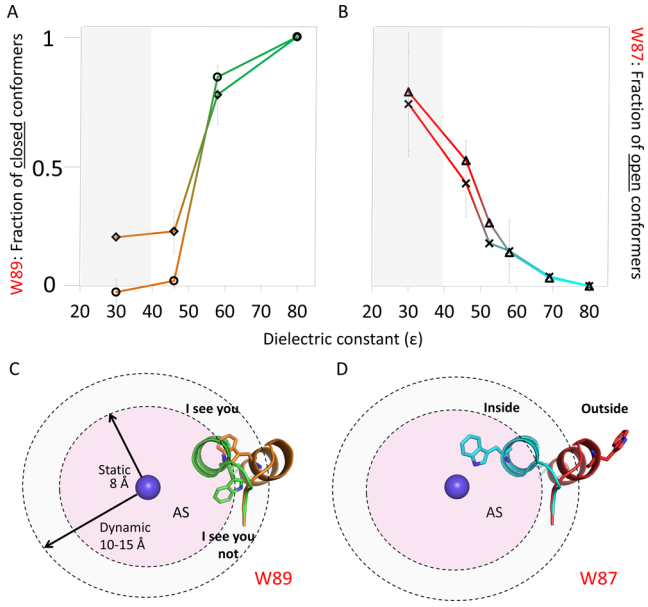

Figure 8. "Activation plots" showing the fraction of lipase conformers as a function of dielectric constant. The plot reports the changes observed at different solvent mixtures for variants with the Trp residue at (A) position 89 (green/yellow gradient lines; diamonds, Lipase_W89; circles, Hybrid_W89) and (B) position 87 (red/cyan gradient lines; triangles, Lipase_W87; crosses, Hybrid_W87) in the lid. Structures of the open/closed states of the lid in variants with Trp at (C) position 89 (yellow/green α-helix and Trp residue, respectively) and (D) position 87 (red/cyan α-helix and Trp residue, respectively). The bimane's empirically determined potential "sphere of quenching",[27] which represents the C_α–C_α distances between the bimane labeling site (blue sphere) and Trp within which static (pink sphere) and dynamic (gray sphere) quenching can occur, respectively, is also shown. For variants with Trp at position 89, lipase activation occurs according to the "I see you, I see you not" phenomenon, where the Trp is pointing into the active site (AS) crevice and upon lid opening confronts the bimane probe attached to site C255, resulting in more quenching. For variants with Trp at position 87, lipase activation occurs according to the "inside, outside" phenomenon where Trp interacts intimately with the bimane fluorophore in the closed state and upon opening moves outside bimane's sphere of quenching. Error bars denote the standard deviation. PDB entries for closed and open conformations of 1DT3 and 1EIN, respectively.[53] Data and equations used for determining the open/closed fractions of conformers are given in eqs 3 and 4 of the Supporting Information.

Mechanistically, this hypothesis would suggest that the ethanol microaggregates act as an interface for the lipase and trigger activation.

Lipase activation in organic solvents has been given much attention in both *in vitro* and *in silico* studies.[20,45,49−51] It has been shown that the fungal lipase from *Mucor circinelloides* does not undergo a conformational change of the lid from a closed to an open state in pure toluene.[20] Interestingly, the conformational change occurred only when a polar substance was added. To explain this observation, it was proposed that the polar additive generates hydrogen bonds with the Trp residue in the lid, thereby facilitating formation of the open lid conformation.[20] For TL lipase, *in silico* studies have shown a partial opening of the lid in pure toluene during a 25 ns simulation.[45] However, the opening was not complete. These results agree well with the results from this study, showing that a full transition from the closed to the open state happens preferably in the presence of a polar, hydrogen bonding substance, e.g., a monohydric alcohol.

Finally, we note that to study the differences between TL lipase and the lid variants, future experiments could be conducted in nonpolar, aprotic solvents such as toluene, hexane, and dioxane. However, as stressed by Klibanov and Zaks, to maintain the catalytic activity and conformational flexibility of the protein, a polar substance must be present.[52] Hence, upon selection of a proper solvent mixture for studying lipase activation as a function of dielectric constant, considerations of the impact of a low dielectric constant on the conformational flexibility of the protein are highly important.

CONCLUSION

Our investigation into the activation mechanism of TL lipase, and lipase lid variants containing FAEA characteristics, shows that it is possible to deduce the open/closed conformational states of the lid in a homogeneous aqueous solution using the TrIQ method. The results suggest that the lid is in an open, activated form for Esterase_W89 containing a lid with FAEA characteristics. In contrast, for Lipase_W89, Hybrid_W89, Lipase_W87 and Hybrid_W87, the lid seems to be in a closed conformation, a conclusion supported by the surface-exposed hydrophobic surface area detected using ANS. Importantly, we have shown that it is possible to detect structural activation of the lid in TL lipase as a function of solvent polarity. Furthermore, our data suggest that Hybrid_W89 activates more favorably in polar solutions than Lipase_W89, in accordance with previous studies. This has interesting ramifications for creating novel lipases with faster activation at the water−lipid interface in an aqueous solution. To gain a better understanding of the activation mechanism of TL lipase, future experiments should focus on using the TrIQ method to study lipases in more native environments, such as in the

DOI: 10.1021/acs.biochem.5b00328
Biochemistry 2015, 54, 4186−4196

presence of lipids and micelles, as well as determining lid opening energy landscapes using *in silico* methods.

■ ASSOCIATED CONTENT

Supporting Information

A figure showing a primary sequence alignment of the lid regions in the studied variants, a table of the theoretically calculated and detected molecular weights of each untreated, reduced, and bimane-labeled variant using LC−ESI-MS, a figure of the peaks detected for untreated, reduced, and bimane-labeled Lipase_W87, a figure showing the absorbance spectra of each labeled variant, a figure showing the fluorescence emission spectra of a selection of variants to indicate the amount of free label, a table showing the values used for calculating the dielectric constant in different water/ethanol mixtures, a table showing the data from the average fluorescence $\langle\tau\rangle$ lifetime measurements, a figure showing the raw far-UV CD spectra for certain variants in different water/ethanol mixtures, a table showing the values of the ANS fluorescence emission maxima detected for each sample, a figure showing the thermal stability of each variant before and after labeling, a figure showing the lipase activity of each variant before and after labeling, and a table and equations showing the values used to calculate the fraction of open and closed conformers for each variant as a function of solvent polarity. The Supporting Information is available free of charge on the ACS Publications website at DOI: 10.1021/acs.biochem.5b00328.

■ AUTHOR INFORMATION

Corresponding Author

*Universitetsparken 5, 2100 København Ø, Denmark. Telephone: +4529260452. E-mail: mobj@chem.ku.dk.

Funding

This work was funded by the industrial PhD program EFU:Novozymes (12-128740 and 0604-01457B). This work was also supported by National Institutes of Health Grants EY015436 and S10RR025684 (to D.F.).

Notes

The authors declare no competing financial interest.

■ ACKNOWLEDGMENTS

We thank the researchers at the R&D facilities at Novozymes for assistance. We give special thanks to Christian Isak Jørgensen from Novozymes and Amber Jones Brunette, Christopher Shafer, and Jonathan Fay from the Oregon Health & Science University.

■ ABBREVIATIONS

FAEA, ferulic acid esterase from *A. niger*; TL, *T. lanuginosus*; TrIQ, tryptophan-induced quenching; SDFL, site-directed fluorescence labeling; pNP, *p*-nitrophenol; ANS, 1-anilinonaphthalene-8-sulfonic acid; CD, circular dichroism; FRET, Förster resonance energy transfer.

■ REFERENCES

(1) Brady, L., Brzozowski, A. M., Derewenda, Z. S., Dodson, E., Dodson, G., Tolley, S., Turkenburg, J. P., Christiansen, L., Huge-Jensen, B., Norskov, L., Thim, L., and Menge, U. (1990) A serine protease triad forms the catalytic centre of a triacylglycerol lipase. *Nature 343*, 767−770.

(2) Brzozowski, A. M., Derewenda, U., Derewenda, Z. S., Dodson, G. G., Lawson, D. M., Turkenburg, J. P., Bjorkling, F., Huge-Jensen, B., Patkar, S. A., and Thim, L. (1991) A model for interfacial activation in lipases from the structure of a fungal lipase-inhibitor complex. *Nature 351*, 491−494.

(3) Derewenda, U., Swenson, L., Wei, Y., Green, R., Kobos, P. M., Joerger, R., Haas, M. J., and Derewenda, Z. S. (1994) Conformational lability of lipases observed in the absence of an oil-water interface: Crystallographic studies of enzymes from the fungi *Humicola lanuginosa* and *Rhizopus delemar*. *J. Lipid Res. 35*, 524−534.

(4) Lawson, D. M., Brzozowski, A. M., Rety, S., Verma, C., and Dodson, G. G. (1994) Probing the nature of substrate binding in *Humicola lanuginosa* lipase through X-ray crystallography and intuitive modelling. *Protein Eng. 7*, 543−550.

(5) Sarda, L., and Desnuelle, P. (1958) Action de la lipase pancrèatique sur les esters en èmulsion. *Biochim. Biophys. Acta 30*, 513−521.

(6) Skjold-Joergensen, J., Vind, J., Svendsen, A., and Bjerrum, M. J. (2014) Altering the Activation Mechanism in Thermomyces lanuginosus Lipase. *Biochemistry 53*, 4152−4160.

(7) Shu, Z., Duan, M., Yang, J., Xu, L., and Yan, Y. (2009) *Aspergillus niger* lipase: Heterologous expression in *Pichia pastoris*, molecular modeling prediction and the importance of the hinge domains at both sides of the lid domain to interfacial activation. *Biotechnol. Prog. 25*, 409−416.

(8) Shu, Z., Wu, J., Xue, L., Lin, R., Jiang, Y., Tang, L., Li, X., and Huang, J. (2011) Construction of *Aspergillus niger* lipase mutants with oil−water interface independence. *Enzyme Microb. Technol. 48*, 129−133.

(9) Yu, X. W., Zhu, S. S., Xiao, R., and Xu, Y. (2014) Conversion of a *Rhizopus chinensis* Lipase into an Esterase by Lid Swapping. *J. Lipid Res. 55*, 1044−1051.

(10) Brzozowski, A. M., Savage, H., Verma, C. S., Turkenburg, J. P., Lawson, D. M., Svendsen, A., and Patkar, S. (2000) Structural Origins of the Interfacial Activation in *Thermomyces* (*Humicola*) *lanuginosa* Lipase. *Biochemistry 39*, 15071−15082.

(11) Norin, M., Olsen, O., Svendsen, A., Edholm, O., and Hult, K. (1993) Theoretical studies of *Rhizomucor miehei* lipase activation. *Protein Eng. 6*, 855−863.

(12) Peters, G. H., Toxvaerd, S., Olsen, O. H., and Svendsen, A. (1997) Computational studies of the activation of lipases and the effect of a hydrophobic environment. *Protein Eng. 10*, 137−147.

(13) Peters, G. H., Olsen, O. H., Svendsen, A., and Wade, R. C. (1996) Theoretical investigation of the dynamics of the active site lid in *Rhizomucor miehei* lipase. *Biophys. J. 71*, 119−129.

(14) Hedin, E. M. K., Høyrup, P., Patkar, S. A., Vind, J., Svendsen, A., and Hult, K. (2005) Implications of Surface Charge and Curvature for the Binding Orientation of *Thermomyces lanuginosus* Lipase on Negatively Charged or Zwitterionic Phospholipid Vesicles As Studied by ESR Spectroscopy. *Biochemistry 44*, 16658−16671.

(15) Ranaldi, S., Belle, V., Woudstra, M., Rodriguez, J., Guigliarelli, B., Sturgis, J., Carriere, F., and Fournel, A. (2009) Lid Opening and Unfolding in Human Pancreatic Lipase at Low pH Revealed by Site-Directed Spin Labeling EPR and FTIR Spectroscopy. *Biochemistry 48*, 630−638.

(16) Ranaldi, S., Belle, V., Woudstra, M., Bourgeas, R., Guigliarelli, B., Roche, P., Vezin, H., Carrière, F., and Fournel, A. (2010) Amplitude of Pancreatic Lipase Lid Opening in Solution and Identification of Spin Label Conformational Subensembles by Combining Continuous Wave and Pulsed EPR Spectroscopy and Molecular Dynamics. *Biochemistry 49*, 2140−2149.

(17) Jutila, A., Zhu, K., Tuominen, E. K. J., and Kinnunen, P. K. J. (2004) Fluorescence spectroscopic characterization of *Humicola lanuginosa* lipase dissolved in its substrate. *Biochim. Biophys. Acta 1702*, 181−189.

(18) Stobiecka, A., Wysocki, S., and Brzozowski, A. M. (1998) Fluorescence study of fungal lipase from *Humicola lanuginosa*. *J. Photochem. Photobiol., B 45*, 95−102.

DOI: 10.1021/acs.biochem.5b00328
Biochemistry 2015, 54, 4186−4196

(19) Yapoudjian, S., Ivanova, M. G., Brzozowski, A. M., Patkar, S. A., Vind, J., Svendsen, A., and Verger, R. (2002) Binding of *Thermomyces* (*Humicola*) *lanuginosa* lipase to the mixed micelles of cis-parinaric acid/NaTDC: Fluorescence resonance energy transfer and crystallographic study. *Eur. J. Biochem. 269*, 1613−1621.
(20) Antczak, T., Graczyk, J., Szczesna-Antczak, M., and Bielecki, S. (2002) Activation of *Mucor circinelloides* lipase in organic medium. *J. Mol. Catal. B: Enzym. 19*−*20*, 287−294.
(21) Brocca, S., Secundo, F., Ossola, M., Alberghina, L., Carrea, G., and Lotti, M. (2003) Sequence of the lid affects activity and specificity of *Candida rugosa* lipase isoenzymes. *Protein Sci. 12*, 2312−2319.
(22) Secundo, F., Carrea, G., Tarabiono, C., Gatti-Lafranconi, P., Brocca, S., Lotti, M., Jaeger, K. E., Puls, M., and Eggert, T. (2006) The lid is a structural and functional determinant of lipase activity and selectivity. *J. Mol. Catal. B: Enzym. 39*, 166−170.
(23) Derewenda, U., Brzozowski, A. M., Lawson, D. M., and Derewenda, Z. S. (1992) Catalysis at the interface: The anatomy of a conformational change in a triglyceride lipase. *Biochemistry 31*, 1532−1541.
(24) McAuley, K. E., Svendsen, A., Patkar, S. A., and Wilson, K. S. (2004) Structure of a feruloyl esterase from *Aspergillus niger*. *Acta Crystallogr. D60*, 878−887.
(25) Aliwan, F. O., Kroon, P. A., Faulds, C. B., Pickersgill, R., and Williamson, G. (1999) Ferulic acid esterase-III from *Aspergillus niger* does not exhibit lipase activity. *J. Sci. Food Agric. 79*, 457−459.
(26) Stryer, L., and Haugland, R. P. (1967) Energy transfer: A spectroscopic ruler. *Proc. Natl. Acad. Sci. U.S.A. 58*, 719−726.
(27) Mansoor, S. E., DeWitt, M. A., and Farrens, D. L. (2010) Distance Mapping in Proteins Using Fluorescence Spectroscopy: The Tryptophan-Induced Quenching (TrIQ) Method. *Biochemistry 49*, 9722−9731.
(28) Jones Brunette, A. M., and Farrens, D. L. (2014) Distance Mapping in Proteins Using Fluorescence Spectroscopy: Tyrosine, like Tryptophan, Quenches Bimane Fluorescence in a Distance-Dependent Manner. *Biochemistry 53*, 6290−6301.
(29) Kosower, E. M., and Huppert, D. (1986) Excited State Electron and Proton Transfers. *Annu. Rev. Phys. Chem. 37*, 127−156.
(30) Doose, S., Neuweiler, H., and Sauer, M. (2005) A Close Look at Fluorescence Quenching of Organic Dyes by Tryptophan. *ChemPhysChem 6*, 2277−2285.
(31) Ho, S. N., Hunt, H. D., Horton, R. M., Pullen, J. K., and Pease, L. R. (1989) Site-directed mutagenesis by overlap extension using the polymerase chain reaction. *Gene 77*, 51−59.
(32) Christensen, T., Woeldike, H., Boel, E., Mortensen, S. B., Hjortshoej, K., Thim, L., and Hansen, M. T. (1988) High Level Expression of Recombinant Genes in *Aspergillus oryzae*. *Nat. Biotechnol. 6*, 1419−1422.
(33) Vind, J. Constructing and screening a DNA library of interest in filamentous fungal cells. WO200024883, 1999.
(34) Hedin, E. M., Patkar, S. A., Vind, J., Svendsen, A., Hult, K., and Berglund, P. (2002) Selective reduction and chemical modification of oxidized lipase cysteine mutants. *Can. J. Chem. 80*, 529−539.
(35) Lakowicz, J. R. (2006) *Principles of Fluorescence Spectroscopy*, pp 282−283, Springer, Berlin.
(36) Mansoor, S. E., and Farrens, D. L. (2004) High-Throughput Protein Structural Analysis Using Site-Directed Fluorescence Labeling and the Bimane Derivative (2-Pyridyl)dithiobimane. *Biochemistry 43*, 9426−9438.
(37) Crowther, G. J., Napuli, A. J., Thomas, A. P., Chung, D. J., Kovzun, K. V., Leibly, D. J., Castaneda, L. J., Bhandari, J., Damman, C. J., Hui, R., Hol, W. G. J., Buckner, F. S., Verlinde, C. L. M. J., Zhang, Z., Fan, E., and van Voorhis, W. C. (2009) Buffer Optimization of Thermal Melt Assays of *Plasmodium* Proteins for Detection of Small-Molecule Ligands. *J. Biomol. Screening 14*, 700−707.
(38) Franks, F. (1972) *Water, a comprehensive treatise*, Plenum Press, New York.
(39) Wang, P., and Anderko, A. (2001) Computation of dielectric constants of solvent mixtures and electrolyte solutions. *Fluid Phase Equilib. 186*, 103−122.
(40) Mansoor, S. E., Mchaourab, H. S., and Farrens, D. L. (2002) Mapping proximity within proteins using fluorescence spectroscopy. A study of T4 lysozyme showing that tryptophan residues quench bimane fluorescence. *Biochemistry 41*, 2475.
(41) Stryer, L. (1965) The interaction of a naphthalene dye with apomyoglobin and apohemoglobin: A fluorescent probe of non-polar binding sites. *J. Mol. Biol. 13*, 482−495.
(42) Cajal, Y., Svendsen, A., De Bolos, J., Patkar, S. A., and Alsina, M. A. (2000) Effect of the lipid interface on the catalytic activity andspectroscopic properties of a fungal lipase. *Biochimie 82*, 1053−1061.
(43) Zaks, A., and Klibanov, A. M. (1985) Enzyme-catalyzed processes in organic solvents. *Proc. Natl. Acad. Sci. U.S.A. 82*, 3192−3196.
(44) Fernandez-Lafuente, R. (2010) Lipase from *Thermomyces lanuginosus*: Uses and prospects as an industrial biocatalyst. *J. Mol. Catal. B: Enzym. 62*, 197−212.
(45) Rehm, S., Trodler, P., and Pleiss, J. (2010) Solvent-induced lid opening in lipases: A molecular dynamics study. *Protein Sci. 19*, 2122−2130.
(46) Santini, S., Crowet, J. M., Thomas, A., Paquot, M., Vandenbol, M., Thonart, P., Wathelet, J. P., Blecker, C., Lognay, G., Brasseur, R., Lins, L., and Charloteaux, B. (2009) Study of *Thermomyces lanuginosa* Lipase in the Presence of Tributyrylglycerol and Water. *Biophys. J. 96*, 4814−4825.
(47) Closs, G. L., and Miller, J. R. (1988) Intramolecular Long-Distance Electron Transfer in Organic Molecules. *Science 240*, 440−447.
(48) Onori, G., and Santucci, A. (1996) Dynamical and structural properties of water/alcohol mixtures. *J. Mol. Liq. 69*, 161−181.
(49) Kulschewski, T., Sasso, F., Secundo, F., Lotti, M., and Pleiss, J. (2013) Molecular mechanism of deactivation of *C. antarctica* lipase B by methanol. *J. Biotechnol. 168*, 462−469.
(50) Trodler, P., Schmid, R. D., and Pleiss, J. (2009) Modeling of solvent-dependent conformational transitions in *Burkholderia cepacia* lipase. *BMC Struct. Biol. 9*, 38.
(51) Trodler, P., and Pleiss, J. (2008) Modeling structure and flexibility of *Candida antarctica* lipase B in organic solvents. *BMC Struct. Biol. 8*, 9.
(52) Zaks, A., and Klibanov, A. M. (1988) The effect of water on enzyme action in organic media. *J. Biol. Chem. 263*, 8017−8021.
(53) Delano, W. L. (2002) *The PyMOL Molecular Graphics System*, DeLano Scientific, San Carlos, CA.

DOI: 10.1021/acs.biochem.5b00328
Biochemistry 2015, 54, 4186−4196